Diffusional screening in treelike spaces: An exactly solvable diffusion-reaction model

Michael Mayo,[1,*] Stefan Gheorghiu,[2] and Peter Pfeifer[1]
[1]*Department of Physics and Astronomy, University of Missouri, Columbia, Missouri 65201, USA*
[2]*Center for Complexity Studies, Aleea Parva 5, Bucharest 061942, Romania*
(Received 24 March 2011; published 9 January 2012)

A renormalization approach is used to derive an analytic formula for the total current crossing the reactive surface of a Cayley tree of cylindrical tubes under a Helmholtz-type approximation to the full diffusion-reaction problem. We provide analytic conditions for the emergence of a plateau in the current—a region of maximum insensitivity of the current to variations in either the reaction rate (membrane permeability) or the diffusivity. The occurrence of such a plateau is associated with a partial screening regime wherein most of the active surface is screened to incoming diffusing particles. Large trees trade efficiency for fault tolerance, a valuable feature which may provide robustness to mammalian respiratory systems and tolerance to catalytic poisoning in chemical reactors.

DOI: 10.1103/PhysRevE.85.011115 PACS number(s): 05.70.Np, 05.60.−k, 05.40.Jc, 05.10.Cc

I. INTRODUCTION

Branching treelike structures are commonly found throughout nature, where they are often the geometry of choice for the transport and delivery of vital substances—such as oxygen in mammalian lungs, nutrients and other biomolecules in the vascular system—from a central source to a distributed target. Such space-filling, hierarchical networks have been shown to provide the optimal (e.g., fastest, most uniform, etc.) access from a single point to a service volume for a variety of transport phenomena such as heat conduction, convection, and pressure-driven flow [1]. Moreover, research in engineering and life sciences has revealed that the particular geometry of fractal-like distribution networks provides multiple advantages such as energy efficiency and fault tolerance [2–4], as well as explaining intriguing properties such as allometric scaling [5].

Here we address the problem of molecular diffusion within a treelike structure of tubes, with a source for the diffusing species placed at the entrance of the "trunk" and a concentration-dependent sink along the surface of the tubes. As such, the current study falls within the broad class of diffusion-reaction problems, an active area of research especially within the physics and chemical engineering communities. Several seminal papers [6,7] have provided insight into diffusion and reaction in hierarchical or fractal-like spaces. Notable results from the field of diffusion-reaction in branching geometries include studies of diffusion on Cayley graphs [8–10], as well as trees of tubes [11] and square channels [12]. While most such studies provide recursive results, the present article delivers a closed-form, analytic formula for a diffusion-reaction problem in a treelike space.

Without losing their generality, we claim that our results provide insights into the respiratory physiology of mammalian lungs. As shown by the exhaustive studies of Weibel [13], the physiology of the lung crucially depends on scale. The dominating transport phenomenon in the large-scale bronchi and bronchioles (roughly the first 15–16 generations of branching of the pulmonary tree) is convective flow, driven by the pressure differences generated by respiration. As the bronchial airways bifurcate, their total cross section increases exponentially so that the flow rate vanishes with increasing depth, and stationary diffusion becomes the primary transport mechanism for respiratory gases. The corresponding mesoscale for which this occurs (approximately 1 mm) defines the size of the lung's gas exchange units, clusters of alveolar sacs known as acini [14,15]. These acini host an airway network, beginning with the transitional and respiratory bronchioles (generations 15–18), which connect to a network of alveolar ducts that subdivides acini into 8 subacini (at rest) beginning with generation 18. Any further downward scaling of the airway network ends at the alveolar ducts of these subacini [16], which support the individual alveoli (approximately 200 μm [14,15]) along their sidewalls and end caps. The particular choice of geometry and physics of the present study provide, therefore, a suitable model for the gas exchange at the level of the pulmonary subacinus.

II. THE MODEL

Figure 1 shows an exemplary geometry of a branching pore space addressed by the present study. The surface-scale geometry of the branches is not essential to the main result of this paper, so for simplicity they are considered cylinders. A diffusing species travels from a source at the entrance of the trunk to the boundary of the pore space, where it either reacts (e.g., in a catalytic reaction) or crosses a membrane (e.g., in gas exchange within the lung). Inside the homogeneous pore space, the diffusion-reaction process is modeled by the Laplace equation:

$$\vec{\nabla}^2 C(\vec{x}) = 0, \tag{1}$$

where C is the difference in concentration of the diffusing species between the pore space and its exterior. This concentration is kept constant at the "root" of the tree $C(\vec{x} = 0) = C_0$, while elsewhere on the boundary of the pore space, the bulk

*Environmental Laboratory, US Army Engineer Research and Development Center, Vicksburg, MS 39180, USA; michael.l.mayo@usace.army.mil

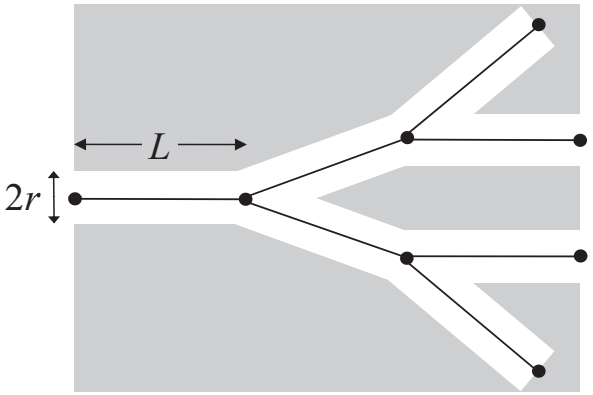

FIG. 1. A model treelike pore space constructed of identical cylindrical branches of radius r and length L. Here the number of daughter branches extending from each parent branch is $m = 2$ while the number of branching generations is $n = 2$. Particles diffuse inside the cylinders and react (or are absorbed) on the cylinder walls.

flux into the boundary is matched to a local rate of destruction of the diffusing species:

$$\vec{\nabla} C(\vec{x}) \cdot \hat{n}(\vec{x}) = \frac{W}{D} C(\vec{x}) \text{ with } \vec{x} \in \text{ boundary}, \tag{2}$$

wherein D is the bulk diffusion coefficient of the diffusing species and the boundary "permeability" W is defined as the number of molecules disappearing at the boundary per unit time, unit area, and unit concentration.

Equation (1) gives an exact representation of single component diffusion or of a species diffusing throughout a binary mixture with equimolar counterdiffusion. For multicomponent mixtures, diffusion of each species is driven by the concentration gradients of all other species, so Eq. (1) is an approximation of the exact Maxwell-Stefan equations, and D may be equated with an effective binary diffusivity of the species under study.

From a chemical engineering viewpoint, boundary condition (2) can be interpreted as a first-order chemical reaction catalyzed on the surface of the pore (e.g., an isomerization reaction), wherein W is the reaction rate coefficient per unit area, related, for example, to the catalytic efficiency of the pore surface. In a biological setting such as the mammalian lung, W is taken to be the membrane permeability to a diffusing species of the acinar gas (for clarity we choose oxygen, O_2). The transport of O_2 from air to blood involves a number of consecutive processes, the rate-limiting step being diffusion through the alveolar membrane and blood plasma, wherein oxygen binds to hemoglobin and the resulting saturation curve is approximately linear for smaller oxygen partial pressures.

Under the assumption that transport of respiratory gases across the lung membrane is mostly passive (unmediated), Katchalsky [17] gave the expression for the diffusional flux into a membrane of thickness δ:

$$J = -D_m \frac{\Delta C}{\delta}, \tag{3}$$

where ΔC is the O_2 concentration difference between the air and blood side. Here D_m is an effective diffusion coefficient for oxygen:

$$D_m = \phi_w R T \beta_{O2} D_{O2}, \tag{4}$$

wherein ϕ_w is the volume fraction of water in the membrane, β_{O2} is Henry's law coefficient for oxygen (the ratio of the concentration of oxygen dissolved in the membrane to the partial pressure of oxygen in air at temperature T [mol/m^3 Pa]), R is the universal gas constant, and D_{O2} is the diffusion coefficient of oxygen within the membrane [m^2/s]. In good approximation, the membrane-plasma system can be considered as a water barrier, so that $\phi_w \approx 1.0$, and D_{O2} and β_{O2} are calculated for oxygen in water. From Eqs. (2)–(4) we may define a permeability for the alveolar membrane:

$$W = \frac{R T \beta_{O2} D_{O2}}{\delta}. \tag{5}$$

Under physiological conditions (low solute concentration/partial pressure), β_{O2} is not dependent on oxygen concentration. Also, at the level of the subacinus, the membrane thickness is roughly constant, so that W is position-independent, although determined by physiology. The generic diffusion-reaction model given by Eqs. (1) and (2) therefore accurately describes gas exchange across the alveolar membranes of the lung, wherein $C(\vec{x})$ should be interpreted as a position-dependent concentration *difference* between the air and the blood side of the alveolar membrane.

Equation (2) defines a characteristic length scale $\Lambda = D/W$, known as the exploration length, which measures the length along the surface that a molecule explores before it reacts [18,19] and which effectively quantifies the diffusional screening of the surface. The diffusion-limited regime is intuitively described by a small exploration length ($\Lambda \to 0$), where the details of a surface's geometry crucially influence reaction rate or molecular transport across it. A large exploration length ($\Lambda \to \infty$) describes the reaction-limited regime, in which all surface details are washed out and only the *total* surface area matters to reaction and/or transport rates.

Using the exploration length as a measure of the surface's accessibility to the diffusing species, we derive a simple, *analytic* formula for the total current crossing the surface of a branching, hierarchical pore space (tree), as well as a formula for the efficiency of such a structure, for example, as a gas exchanger.

III. BRANCH HIERARCHY

A treelike space (Fig. 1) provides an idealized model for a catalyst pore with reactive walls, or for a gas exchange unit (e.g., lung acinus) lined with a membrane permeable to O_2. All branches of the tree are identical cylinders of length L and radius r; each branch bifurcates into m daughter branches for up to n consecutive generations (Fig. 2). Each bifurcation point is called a node; they are labeled from $i = 0$ (the root of the tree) to $i = n + 1$ (the ends of the terminal branches, termed "leaves"). For every branch, labeled by e_i, connecting a node of order i to an adjacent one of order $i + 1$, the values for particle current and concentration at the entrance are denoted

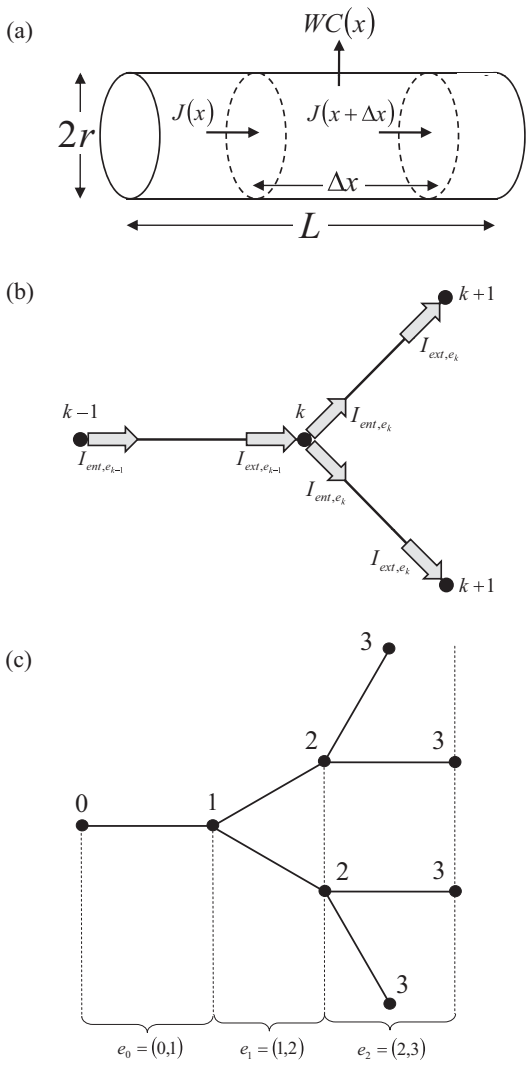

FIG. 2. Elements of the hierarchical model. (a) Mass conservation within a cylindrical branch, leading to a Helmholtz equation for the concentration of the diffusing species. (b) Mass conservation across an exemplary node. (c) Node and branch labeling scheme used throughout the paper.

by I_{ent,e_i} and C_{ent,e_i}, respectively. Similarly, the exit values I_{ext,e_i} and C_{ext,e_i} denote these quantities at node $i+1$.

IV. HELMHOLTZ TREATMENT OF AN INDIVIDUAL BRANCH

In an approximation to Eqs. (1) and (2) that exploits symmetry and ignores radial concentration gradients, mass balance in a branch (shown in Fig. 2) gives a one-dimensional Helmholtz equation:

$$\frac{d^2}{dx^2}C(x) - \left(\frac{\varphi}{L}\right)^2 C(x) = 0, \tag{6}$$

wherein the branch's dimensionless Thiele modulus, φ, is related to the exploration length by

$$\varphi = L\sqrt{\frac{2W}{rD}} = L\sqrt{\frac{2}{r\Lambda}}. \tag{7}$$

The solution of Eq. (6) can be expressed as a function of the concentrations at the nodes,

$$C(x) = \frac{C_{\mathrm{ent}}\sinh\left[\varphi(1-x/L)\right] + C_{\mathrm{ext}}\sinh\left(\varphi x/L\right)}{\sinh\varphi}, \tag{8}$$

as a function of the diffusive currents through the nodes,

$$C(x) = \frac{I_{\mathrm{ent}}\cosh\left[\varphi(1-x/L)\right] - I_{\mathrm{ext}}\cosh\left(\varphi x/L\right)}{(\pi r^2 D/L)\varphi\sinh\varphi}, \tag{9}$$

or finally, as a mixed expression involving node currents and concentrations. Node concentrations are related to their respective currents by

$$\frac{I_{\mathrm{ent}}}{\pi r^2 D} = -\left.\frac{dC}{dx}\right|_{x=0} \quad \text{and} \quad \frac{I_{\mathrm{ext}}}{\pi r^2 D} = -\left.\frac{dC}{dx}\right|_{x=L}, \tag{10}$$

while the current into the branch's reactive surface is given by

$$\Delta I = I_{\mathrm{ent}} - I_{\mathrm{ext}} = \int_0^L WC(x)dx. \tag{11}$$

A renormalization calculation (Appendix B) built from equations of type (8)–(11) yields analytical expressions for the total current and the concentration profile within the tree. The accuracy of this simplified one-dimensional treatment is discussed in Appendix A, where the Helmholtz concentration profile is compared to the exact solution of Laplace's equation (1) in a cylinder.

V. RESULTS

A. Total current into the tree

To the chemical engineer, this current represents the yield of a chemical reaction taking place inside the homogeneous pore space; to the physiologist, this current corresponds to the exchange rate of respiratory gases (e.g., oxygen) within the model acinus. The following expression gives the total current into the tree:

$$I = \frac{\pi r^2 DC_0}{mLg^{n+1}(\Lambda/L)}. \tag{12}$$

Here $C_0 = C_{\mathrm{ent},e_0}$ is the concentration of the diffusing species at the root, while g is an attenuation function of the exploration length,

$$g\left(\frac{\Lambda}{L}\right) = \frac{\left(\frac{\Lambda}{L}\right)\varphi + \tanh\varphi}{\left(\frac{\Lambda}{L}\right)m\varphi^2\tanh\varphi + m\varphi}, \tag{13}$$

and the $n+1$st power of g is computed as $n+1$-fold function composition: $g^{n+1}(\cdot) = g\circ\cdots\circ g(\cdot)$. Details of the renormalization calculation leading to Eqs. (12) and (13) are provided in Appendix B.

The attenuation function g, seen as a function of the dimensionless exploration length Λ/L, can be interpreted as a Möbius transformation of the complex plane. It can then be shown that the k-fold composition of g can be evaluated by calculating the kth power of a dimensionless Möbius matrix [20],

$$G = \begin{pmatrix} \varphi & \tanh\varphi \\ m\varphi^2\tanh\varphi & m\varphi \end{pmatrix}, \tag{14}$$

which can be carried out by matrix diagonalization to yield

$$g^{n+1}\left(\frac{\Lambda}{L}\right)=\frac{\frac{\sinh\varphi}{\varphi}+\frac{2L}{r\varphi^2}\left(\frac{1}{2}[(1-m)\cosh\varphi+\sqrt{\cdot}]+\frac{\sqrt{\cdot}}{\left[\frac{1}{4m}((1+m)\cosh\varphi+\sqrt{\cdot})^2\right]^{n+1}-1}\right)}{\frac{2mL\sinh\varphi}{r\varphi}-\frac{1}{2}[(1-m)\cosh\varphi-\sqrt{\cdot}]+\frac{\sqrt{\cdot}}{\left[\frac{1}{4m}((1+m)\cosh\varphi+\sqrt{\cdot})^2\right]^{n+1}-1}}. \tag{15}$$

Here we have abbreviated

$$\sqrt{\cdot}=\sqrt{[(1+m)\cosh\varphi]^2-4m}.$$

Expression (15) is exact for sufficiently large exploration length ($r/\Lambda<1$), where the Helmholtz approximation holds.

Figure 3 shows the dimensionless current $1/mg^{n+1}(\Lambda/L)$ plotted against the trunk's Thiele modulus for varying size. In the diffusion-limited regime ($\varphi\to\infty$), diffusing particles only explore the entrance tube (trunk); therefore, all curves collapse onto one describing diffusion and reaction in a cylinder. At the other end, in the reaction-limited regime ($\varphi\to 0$), the current is proportional to the total area of the tree.

We note the branch-by-branch renormalization calculation leading to Eq. (15) can be adapted to include scaling ratios between parent and daughter branches [21]. Given such ratios between successive branch lengths and widths, $p=L_{e_{i+1}}/L_{e_i}$ and $q=r_{e_{i+1}}/r_{e_i}$, respectively, a similar renormalization calculation, as used for branches of equal width and length described in Appendix B, but including these ratios, leads to a p,q-dependent Möbius matrix, which does not generally give analytical results unless $p=q=1$ (although the condition $p=\sqrt{q}$ is a possible exception). This situation ($p=q=1$) is the most biologically relevant, as the "hardware" of mammalian acini conform to this equilength and -width scheme [16]. For this reason, we restrict our discussions here to the equilength and- width case, $p=q=1$.

B. Current plateau

In between the diffusion-limited and the reaction-limited regimes, the current goes through a flat region defined by $\partial I/\partial\varphi=0$, which persists across many orders of magnitude of the Thiele modulus, depending on the geometry of the tree. Such insensitivity of the current to variations in either the reaction rate or the diffusivity is a valuable feature, providing robustness to the respiratory system of mammals, as well as tolerance to catalyst poisoning or deactivation in chemical engineering applications. This type of behavior was observed before in similar diffusion-reaction systems [11,15,22,23], but here it is quantified analytically.

For large exploration length, the current Eq. (15) may be approximated as

$$\frac{1}{mg^{n+1}(\Lambda/L)}\sim\frac{\frac{2L}{r}+\frac{m-1}{m}}{1+\frac{2L}{r}\frac{m}{m-1}+\frac{m-1}{m^{n+1}-1}\left(\frac{\Lambda}{L}\right)}. \tag{16}$$

Further manipulation yields

$$\frac{1}{mg^{n+1}(\Lambda/L)}\sim\frac{\frac{m-1}{m}}{1+\frac{m-1}{m}\frac{\pi r^2}{S_{\text{tree}}}\left(\frac{\Lambda}{L}\right)}, \tag{17}$$

wherein $S_{\text{tree}}=2\pi rL(m^{n+1}-1)/(m-1)+m^n\pi r^2$ is the total surface area of the tree. In the $\varphi\to 0$ limit, Eq. (17) gives the correct asymptote, with the current scaling as the total surface area. A plateau develops when $S_{\text{tree}}/\pi r^2\gg 1$, allowing the second term of the denominator to remain negligible for a wide range of exploration lengths. The low-φ limit of the plateau is given approximately by

$$\varphi=\sqrt{\frac{2\pi rL}{S_{\text{tree}}}},\quad\text{or}\quad\frac{\pi r^2}{S_{\text{tree}}}\left(\frac{\Lambda}{L}\right)=1. \tag{18}$$

The height of the plateau is given by $(m-1)/m$, a result confirmed by Figs. 3 and 4.

The condition $S_{\text{tree}}/\pi r^2\gg 1$ has an elegant intuitive interpretation: A plateau in the current occurs in a system in which a large surface area is accessible through a relatively narrow entrance. In other words, in the plateau region of process parameters, a large proportion of the surface is *screened* to incoming particles. With their ability to pack large surface areas into small volumes, fractal-like objects provide good candidates (although not the only ones) for this type of behavior.

Equation (17) has a very simple form,

$$I\propto\frac{A}{1+B\Lambda}, \tag{19}$$

wherein A and B are functions of geometry alone, while the exploration length Λ quantifies all the information about process parameters. In the partial screening (plateau) regime,

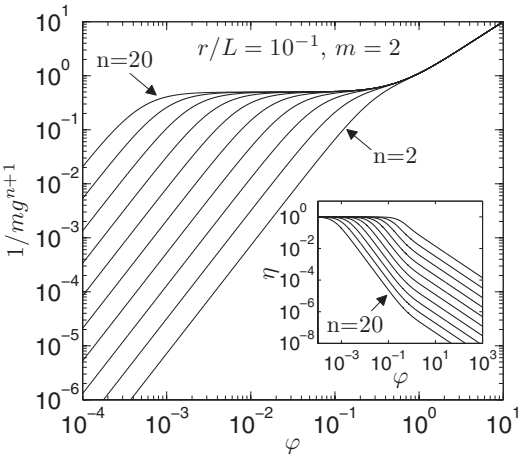

FIG. 3. Total (cumulative) current (dimensionless) for the Cayley tree model as a function of the trunk's Thiele modulus, shown for several trees with fixed branch aspect ratio r/L, fixed number of daughter branches $m=2$, and varying branching generation n. (Inset) Effectiveness factors for the corresponding trees shown.

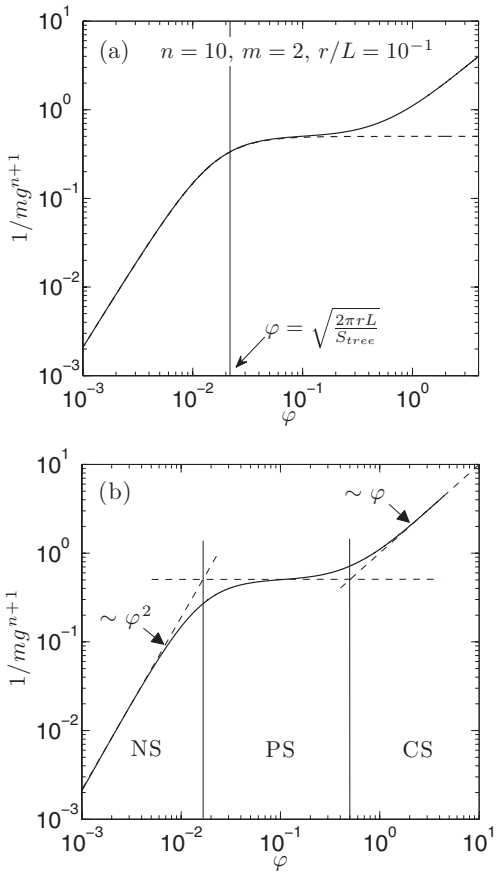

FIG. 4. (a) An exemplary current plateau described by the asymptotic approximation [Eq. (17)] (dashed line). (b) Illustration of the three screening regimes for the tree: no screening (NS), partial screening (PS), or complete screening (CS).

Eq. (19) is noninvertible, in the sense that given the current I, one cannot uniquely determine the trunk's Thiele modulus φ, or the process parameters D and W, for that matter. Thus, partially screened diffusion-reaction systems may pose particular experimental challenges.

Figure 3 further shows that in partial screening, the current is also rather insensitive to the pore network (e.g., to n). In other words, even when Λ is known, the current does not univocally determine the geometry of the pore space; many different trees of tubes produce approximately the same total current I.

The notion that this insensitivity is generated by screening of the active zones suggests it is not restricted to trees. For example, diffusive currents transported across fractal surfaces display similar "robustness" [15]. This should be contrasted with the case of bimodal pore distributions for porous (first-order) catalytic reactors [24,25]: Local variations in the pore diameters and porosity do not significantly improve the current when compared to pore networks maximizing the reaction yield (i.e., the optimized ones).

C. Effectiveness factor and effective surface area of the tree

An effectiveness factor for the tree is defined as the ratio of the total current to the current in the absence of diffusion limitations [12], quantifying the performance of the pore surface as a reactor/gas exchanger:

$$\eta = \frac{W\int_{\text{tree}} C\,dS}{WC_0S_{\text{tree}}} = \frac{I}{WC_0S_{\text{tree}}} = \frac{S_{\text{eff}}}{S_{\text{tree}}}. \tag{20}$$

Equation (20) also defines an "effective" area of the pore, S_{eff}, that is, the area of an equivalent pore which produces the same current in the absence of diffusion limitations. Following Eq. (12), the tree's effective surface area is $S_{\text{eff}} = \pi r^2\Lambda/mLg^{n+1}(\Lambda/L)$, and its effectiveness factor is given by

$$\eta = \frac{\pi r^2}{S_{\text{tree}}}\left[\frac{\Lambda/L}{mg^{n+1}(\Lambda/L)}\right]. \tag{21}$$

The effectiveness factors of several trees are shown in the inset in Fig. 3. The most efficient trees are those with either the smallest number of branch generations n or number of daughter branches m (small to moderate screening). A similar conclusion relating small trees to high efficiencies has been reported for another model of a human lung acinus [3].

This change in efficiency provides a major advantage to mammalian lungs under variable breathing conditions and may be another determining reason for the treelike design of the acinar airways. The transition from convection to diffusion is pushed deeper into the lung as a result of exercise, from about the 18th branching generation at rest to the 21st generation under maximum exercise [2,13]. As a result, the oxygen "source" is pushed deeper into the treelike structure, activating previously inactive surface area for the gas exchange, therefore drastically increasing the current and efficiency; plateaus in the current indicative of robustness are eliminated as this efficiency increases. The lung's ability to accommodate moderate alterations to the membrane's permeability, resulting from changing physiological conditions, is traded for an increased transport efficiency to help meet the body's increasing oxygen demands. So, mammalian lungs pay a high price for increasing efficiency between rest and exercise, in that they are less able to adapt to stress, becoming more "fragile." A tradeoff between robustness and fragility is ubiquitous among other forms of biological regulation [26].

D. The tree as an effective medium

In what can be seen as an effective medium approximation of the tree, the tree is shown to behave as an equivalent tube, or an equivalent patch of reactive surface with appropriately rescaled values of the reaction rate. From Eq. (B5) of the Appendix, the current into a terminal tube may be expressed as

$$I_{\text{ent}} = \frac{D\pi r^2 C_{\text{ent}}}{mLg^{n+1}(\Lambda/L)}. \tag{22}$$

In view of Eq. (22) and Eq. (12) can be rewritten as

$$I = \frac{D\pi r^2 C_0}{mLg\left(\Lambda_{\text{eff}}^{\text{tube}}/L\right)}; \tag{23}$$

that is, the tree behaves like a single branch (the "trunk") with an effective exploration length defined by

$$\frac{\Lambda_{\text{eff}}^{\text{tube}}}{L} = g^n \left(\frac{\Lambda}{L}\right). \tag{24}$$

Rescaling the exploration length corresponds to rescaling the reaction rate (or membrane permeability) W to a much higher value and leads therefore to stronger diffusion limitations: $\varphi_{\text{eff}}^{\text{tube}} \gg \varphi$. Concentration profiles in the equivalent tube decrease more steeply than in the actual tree, resulting in a significantly smaller penetration depth of the diffusing particles. Similarly, Eq. (12) reveals that the tree works as an equivalent patch of reactive surface with area (the root), with an effective exploration length defined by

$$\frac{\Lambda_{\text{eff}}^{\text{patch}}}{L} = m g^{n+1} \left(\frac{\Lambda}{L}\right). \tag{25}$$

VI. CONCLUSIONS

A diffusion-reaction problem was solved in a Cayley tree of cylindrical tubes, modeling a branched catalytic pore, or a gas exchange unit of the lung (acinus). A renormalization approach was shown to provide analytical expressions for the concentration profile, the particle current, and the effectiveness factor for the tree of tubes.

Trees with a large surface area (e.g., a large number of branch generations n) feature a current plateau, a range of moderate surface reactivity wherein the current across the tree's surface depends only weakly, if at all, on the Thiele modulus of the entrance branch (equivalently, the exploration length). This phenomenon coincides with a *partial screening* regime, wherein a significant portion (but not all) of the surface of the tree is screened from access by incoming diffusing particles. Insensitivity of the current with respect to surface reactivity may translate into major advantages, such as tolerance to catalyst deactivation, or robustness of a lung gas-exchange unit against pollution, damage, and disease.

APPENDIX A: VALIDITY OF THE HELMHOLTZ APPROACH

The Helmholtz treatment of individual branches, Eq. (6), ignores any radial dependence of the concentration. Here we show a comparison between the Helmholtz approximation and the exact solution of the Laplace equation, Eq. (1), in a single cylindrical tube to reveal the limits of the model's applicability.

If we provide reflecting boundary conditions at the deep end of the tube, and a constant concentration across its entrance,

$$\left.\frac{dC}{dx}\right|_{x=L} = 0 \text{ and } C(r,x)|_{x=0} = C_{\text{ent}},$$

respectively, then a solution to Eq. (1) is

$$C(\rho,x) = \frac{2rC_{\text{ent}}}{\Lambda} \sum_{i=1}^{\infty} \frac{J_0\left(\delta_i \frac{\rho}{r}\right) \cosh\left(\delta_i \frac{L-x}{r}\right)}{J_0(\delta_i) \cosh\left(\delta_i \frac{L}{r}\right)\left(\delta_i^2 + \left(\frac{r}{\Lambda}\right)^2\right)}. \tag{A1}$$

Here J_0 are Bessel functions of the first kind, and δ_i labels the ascending positive roots of

$$\delta_i J_1(\delta_i) - \frac{r}{\Lambda} J_0(\delta_i) = 0. \tag{A2}$$

The same boundary conditions result in a corresponding solution to the Helmholtz equation, Eq. (6):

$$C(x) = C_{\text{ent}} \frac{\cosh\left[\varphi\left(1 - \frac{x}{L}\right)\right]}{\cosh\varphi}. \tag{A3}$$

The Helmholtz solution, Eq. (A3), is a good approximation of Eq. (A1) if Eq. (A1) is radially independent, that is, if the term $J_0(\delta_i \rho/r)$ is approximately constant for all values of the radial coordinate $0 \leqslant \rho \leqslant r$. Since the concentration of the diffusing species varies only slowly at length scales equal to the exploration length [15,18,19], we expect any radial gradient to vanish as the exploration length approaches the radius of the cylinder. Indeed, an approximation for the first root of Eq. (A2),

$$\delta_1 \approx \sqrt{\frac{2r}{\Lambda}}\left[1 + \frac{1}{8}\left(\frac{r}{\Lambda}\right) + \frac{3}{64}\left(\frac{r}{\Lambda}\right)^2 + \cdots\right],$$

gives $\delta_1 \approx \sqrt{2r/\Lambda} = \varphi r/L$ for $r/\Lambda < 1$. Under this condition we have $J_0(\delta_1 \rho/r) \approx J_0(\delta_1) \approx 1$, and we can rewrite Eq. (A1) as

$$C(\rho,x) \approx C_{\text{ent}} \frac{\cosh\left[\varphi\left(1 - \frac{x}{L}\right)\right]}{\cosh\varphi} + \frac{2rC_{\text{ent}}}{\Lambda} \sum_{i=2}^{\infty} \frac{J_0\left(\delta_i \frac{\rho}{r}\right) \cosh\left(\delta_i \frac{L-x}{r}\right)}{J_0(\delta_i) \cosh\left(\delta_i \frac{L}{r}\right)\left[\delta_i^2 + \left(\frac{r}{\Lambda}\right)^2\right]}. \tag{A4}$$

The leading term of Eq. (A4) coincides with the Helmholtz solution (A3), confirming that the Helmholtz approach used throughout the paper is accurate in the domain of reasonably small Thiele moduli φ (i.e., $r/\Lambda < 1$). The result is confirmed numerically in Fig. 5.

In the opposite limit of high Thiele modulus ($\Lambda \to 0$), the problem of diffusion and reaction in a treelike space is irrelevant, since the diffusing species practically never penetrate beyond the entrance branch (refer to the collapse of all curves into a single one shown in Fig. 3).

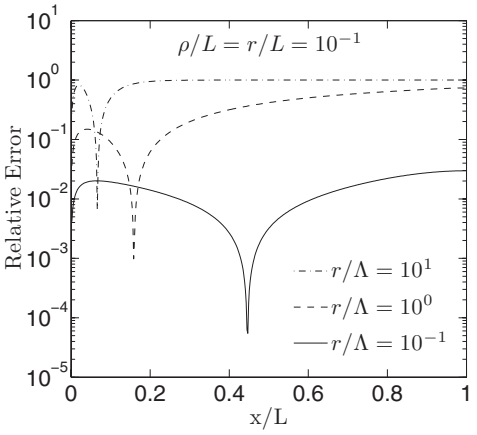

FIG. 5. Relative error between concentrations calculated using the Helmholtz and Laplace (evaluated at $\rho = r$, and truncated at $n = 100$ terms) descriptions of the diffusion-reaction problem, across a single cylindrical pore, for various values of the ratio r/Λ.

APPENDIX B: RENORMALIZATION CALCULATION FOR DIFFUSION CURRENT IN A BRANCHED TREE

We view the Cayley tree model as composed of three classes of tubes: an entrance tube (i.e., trunk), m^n-many terminal tubes, and "intermediate" tubes residing between the trunk and the terminal tubes of the tree. We begin at the "end" of the tree and work our way up to the trunk, which allows the current entering the trunk to be found exactly.

To proceed, we first define the concentration profile within a given terminal branch. The tips of these terminal branches compose a canopy of reactive surface area; we specify the current leaving through the reactive surface of these tips is given by

$$I_{\text{ext},e_n} = \pi r^2 W C_{\text{ext},e_n} = \frac{D\pi r^2}{L\left(\frac{\Lambda}{L}\right)} C_{\text{ext},e_n}. \tag{B1}$$

At the entrance of a terminal branch we give the current that enters it:

$$\left.\frac{dC}{dx}\right|_{x=0} = -\frac{I_{\text{ent},e_n}}{\pi r^2 D}. \tag{B2}$$

Equations (B1) and (B2) *define* the terminal branches. The intermediate branches are defined by specifying the current entering/leaving through the open ends, and the trunk is defined by providing its entrance concentration, C_{ent,e_0}, and the current leaving through its open end. For example, the solution of Eq. (6) for an intermediate branch is given by Eq. (9)

Solving Eq. (6) with conditions (B1) and (B2) gives the following relationships:

$$C_{\text{ent},e_n} = \frac{L\left[I_{\text{ent},e_n}\sinh(\varphi) + \left(\frac{\Lambda}{L}\right)\varphi I_{\text{ext},e_n}\right]}{\varphi\pi r^2 D\cosh\varphi}, \quad \text{and} \tag{B3}$$

$$I_{\text{ent},e_n} = \left[\cosh\varphi + \left(\frac{\Lambda}{L}\right)\varphi\sinh\varphi\right] I_{\text{ext},e_n}. \tag{B4}$$

These equations, Eqs. (B3) and (B4), can be solved to give the current entering a terminal branch:

$$I_{\text{ent},e_n} = \frac{D\pi r^2}{mLg\left(\frac{\Lambda}{L}\right)} C_{\text{ent},e_n}, \tag{B5}$$

wherein the function g involves the Thiele modulus Eq. (7):

$$g\left(\frac{\Lambda}{L}\right) = \frac{\left(\frac{\Lambda}{L}\right)\varphi + \tanh\varphi}{\left(\frac{\Lambda}{L}\right)m\varphi^2\tanh\varphi + m\varphi}. \tag{B6}$$

Now, since $C_{\text{ent},e_n} = C_{\text{ext},e_{n-1}}$ and $I_{\text{ent},e_n} = I_{\text{ext},e_{n-1}}/m$ (conservation of current at node n), Eq. (B5) can be written as

$$I_{\text{ext},e_{n-1}} = \frac{D\pi r^2}{Lg\left(\frac{\Lambda}{L}\right)} C_{\text{ext},e_{n-1}}. \tag{B7}$$

Comparing Eqs. (B1) and (B7), it is clear that we have achieved a renormalization of the problem by transforming a tree with n generations into a tree with $n-1$ generations of branches, the new terminal branches described by a boundary condition given by Eq. (B7). The transformation also rescales the dimensionless exploration length Λ/L to a new exploration length $g(\Lambda/L)$ [e.g., Eqs. (24) and (25)]. By applying the renormalization iteratively to all generations of the tree, one recovers the current entering the root I as a function of its entrance concentration, $C_0 = C_{\text{ent},e_0}$:

$$I = \frac{\pi r^2 D C_0}{mLg^{n+1}\left(\frac{\Lambda}{L}\right)}, \tag{B8}$$

wherein g^{n+1} denotes the $n+1$-fold functional composition $g^{n+1}(\Lambda/L) = g\circ\cdots\circ g\,(\Lambda/L)$.

[1] A. Bejan, Int. J. Heat Mass Transf. **40**, 799 (1997).
[2] C. Hou, S. Gheorghiu, M.-O. Coppens, V. H. Huxley, and P. Pfeifer, in *Fractals in Biology and Medicine Volume IV*, edited by G. A. Losa, D. Merlini, T. F. Nonnenmacher, and E. R. Weibel (Birkhäuser Verlag, Basel, Switzerland, 2005).
[3] B. Sapoval, M. Filoche, and E. R. Weibel, Proc. Natl. Acad. Sci. USA **99**, 10411 (2005).
[4] B. Mauroy, M. Filoche, E. Weibel, and B. Sapoval, Nature (London) **427**, 633 (2004).
[5] G. West, J. Brown, and B. Enquist, Science **276**, 122 (1997).
[6] M. Giona, A. Adrover, W. A. Schwalm, and M. Schwalm, Chem. Eng. Sci. **51**, 5065 (1996).
[7] P. Mougin, M. Pons, and J. Villermaux, Chem. Eng. Sci. **51**, 2293 (1996).
[8] M. Sahimi, Chem. Eng. Sci. **43**, 2981 (1988).
[9] M. Felici, M. Filoche, and B. Sapoval, Phys. Rev. Lett. **92**, 068101 (2004).
[10] M. Felici, M. Filoche, C. Straus, T. Similowski, and B. Sapoval, Respir. Physiol. Neurobiol. **145**, 279 (2005).
[11] M. Sheintuch and S. Brandon, Chem. Eng. Sci. **44**, 69 (1989).
[12] D. S. Grebenkov, M. Filoche, B. Sapoval, and M. Felici, Phys. Rev. Lett. **94**, 050602 (2005).
[13] E. R. Weibel, *The Pathway for Oxygen* (Harvard University Press, Cambridge, MA, 1984).
[14] E. Weibel, B. Sapoval, and M. Filoche, Resp. Phys. Neurobiol. **148**, 3 (2005).
[15] C. Hou, S. Gheorghiu, V. Huxley, and P. Pfeifer, PLoS Comp. Biol. **6**, e1000902 (2010).
[16] B. Haefeli-Bleuer and E. Weibel, Anat. Rec. **220**, 401 (1988).
[17] A. Katchalsky, *Biophysics and Other Topics: Selected Papers* (Academic Press, New York, 1976).
[18] B. Sapoval, Phys. Rev. Lett. **73**, 3314 (1994).
[19] P. Pfeifer and B. Sapoval, Mater. Res. Soc. Symp. Proc. **366**, 271 (1995).
[20] T. Needham, *Visual Complex Analysis* (Oxford University Press, New York, 1997).
[21] M. Mayo, Ph.D. thesis, University of Missouri, 2009.
[22] B. Sapoval, J. S. Andrade, and M. Filoche, Chem. Eng. Sci. **56**, 5011 (2001).
[23] M. Sheintuch, Chem. Eng. Sci. **55**, 615 (2000).
[24] S. Gheorghiu and M.-O. Coppens, AIChE J. **50**, 812 (2004).
[25] G. Wang, E. Johannessen, C. Klein, S. deLeeuw, and M.-O. Coppens, Chem. Eng. Sci. **62**, 5110 (2007).
[26] H. Kitano, Nat. Rev. Genet. **5**, 826 (2004).